MAGNETIC TORQUER ATTITUDE CONTROL VIA ASYMPTOTIC PERIODIC LINEAR QUADRATIC REGULATION

by Mark L. Psiaki[*]

Cornell University, Ithaca, N.Y. 14853-7501

Abstract

A method of using magnetic torque rods to do 3-axis spacecraft attitude control has been developed. The goal of this system is to achieve a nadir pointing accuracy on the order of 0.1 to 1.0 deg without the need for thrusters or wheels. The open-loop system is under-actuated because magnetic torque rods cannot torque about the local magnetic field direction. This direction moves in space as the spacecraft moves along an inclined orbit, and the resulting system is roughly periodic. Periodic controllers are designed using an asymptotic linear quadratic regulator technique. The control laws include integral action and saturation logic. This system's performance has been studied via analysis and simulation. The resulting closed-loop systems are robust with respect to parametric modeling uncertainty. They converge from initial attitude errors of 30 deg per axis, and they achieve steady-state pointing errors on the order of 0.5 to 1.0 deg in the presence of drag torques and unmodeled residual dipole moments.

Introduction

All spacecraft have an attitude stabilization system. They range from passive spin-stabilized [1] or gravity-gradient stabilized [2] systems to fully active three-axis controlled systems [3]. Pointing accuracies for such systems may range from 10 deg down to 10^{-4} deg or better, depending on the spacecraft design and on the types of sensors and actuators that it carries. The most accurate designs normally include momentum wheels or reaction wheels.

This paper develops an active 3-axis attitude stabilization system for a nadir-pointing spacecraft. It uses only magnetic torque rods as actuators. Additional components of the system include appropriate attitude sensors and a magnetometer. The goal of this system is to achieve pointing accuracy that is better than a gravity gradient stabilization system, on the order of 0.1 to 1 deg. Such a system will weigh less than either a gravity-gradient system or a wheel-based system, and it will use less power than a wheel-based system. Thus, it will be ideal for small satellite applications, where weight and power budgets are severely restricted.

There are two classic uses of magnetic torque rods in attitude control. One is for momentum management of wheel-based systems [3]. The other is for angular-momentum and nutation control of spinning [4], momentum-biased [5], and dual-spin spacecraft [6].

The present study is one of a growing number that consider active 3-axis magnetic attitude stabilization of a nadir-pointing spacecraft [7-14]. Reference 5 also should be classified with this group because it uses similar techniques. Reference 7, the earliest such study, presents a 3-axis proportional-derivative control law. It computes a desired torque and projects it perpendicular to the Earth's magnetic field in order to determine the actual torque. Projection is necessary because the magnetic torque, n_m, takes the form

$$n_m = m \times b \qquad (1)$$

where m is the magnetic dipole moment vector of the torque rods and b is the Earth's magnetic field.

Equation (1) highlights the principal problem of magnetic-torque-based 3-axis attitude control: the system is under-actuated. A rigid spacecraft has 3 rotational degrees of freedom, but the torque rods can only torque about the 2 axes that are perpendicular to the magnetic field vector. The system is controllable if the orbit is inclined because the Earth's magnetic field vector rotates in space as the spacecraft moves around its orbit. It is a time-varying system that is approximately periodic. This system's under-actuation and its periodicity combine to create a challenging feedback controller design problem.

The present problem is different from the problem of attitude control when thrusters or reaction wheels provide torque only about 2 axes. References 15 and 16 and others have addressed this alternate problem, in which the un-actuated direction is defined in spacecraft coordinates. For magnetic torques, the un-actuated direction does not rotate with the spacecraft.

Various control laws have been considered for magnetic attitude control systems. Some of the controllers are similar to the original controller of Martel et al. [10,14]. Time-varying Linear Quadratic Regulator (LQR) formulations have been tried [5,8,11], as has fuzzy control [9] and sliding-mode control [12]. References 9 and 13 patch together solutions of time-

---

[*] Associate Professor, Sibley School of Mech. & Aero. Engr. Associate Fellow, AIAA.

invariant LQR problems, solutions that change with time because the "time-invariant" system changes with time.

The present study makes four important contributions to 3-axis magnetic attitude control. First, it develops a time-varying, full-state-feedback LQR control law that is based on a constant approximate solution of the time-varying Riccati equation. Second, it includes integrators in its controller, which counteract the steady-state effects of disturbances. Third, it develops a way to ensure stability in the presence of actuator saturation – this is a first for any time-varying control law. Last, it evaluates the controllers' robustness with respect to parametric model uncertainties.

This paper's approximate LQR solution is similar to the constant gain solution that is presented in Ref. 11. The present development makes a stronger connection to an underlying periodic LQR problem. This connection allows the design to be modified so that it can be guaranteed to remain stable when actuator saturation occurs.

Other studies have considered actuator saturation [9,12] or integral-type controller actions [5]. This is the first paper to consider them together. Simultaneous consideration of these issues is important because integrators can cause stability problems when control saturation occurs.

Some of this paper's results are also applicable to magnetorquer-based attitude control of momentum-bias and spinning spacecraft. Such systems have (almost) periodic models that are similar to those of the present study, and it is possible to design controllers for such systems using the new methods that are presented here.

The body of this paper consists of 3 main sections followed by a short conclusions section. Section 2 presents models of the magnetically controlled attitude dynamics of a nadir-pointing spacecraft. Section 3 develops the theory of asymptotic low-bandwidth periodic linear quadratic regulation, and it explains how to modify the resulting controller in order maintain stability when the control saturates. Section 4 applies the periodic regulator to the magnetic attitude control problem, and it presents analysis and simulation results for the closed-loop system.

II. Models of the Magnetic Attitude Control Problem
Reference Frames and Orbital Model
In the case of a nadir pointing spacecraft, it is traditional to define the vehicle's orientation relative to the local-level coordinate system, which follows the

spacecraft around its orbit. The local-level system's $+z$ axis points towards nadir, and its y axis is perpendicular to both the nadir vector and the instantaneous orbital velocity vector as measured with respect to an Earth-Centered Inertially-Fixed reference frame. The $+y$ axis points towards negative orbit normal. The x axis, defined by the right-hand rule, points approximately along the velocity vector.

The other important reference frame is spacecraft-fixed. When the nadir-pointing spacecraft has the desired attitude, this body-fixed reference frame is aligned with the local-level reference frame. Deviations of this reference frame's attitude from that of the local-level reference frame are parameterized by the attitude quaternion, q. The orthonormal transformation matrix from local-level coordinates to spacecraft coordinates is a function of q: $A_{sc/ll}(q)$ [17].

A model of the spacecraft's orbit is used to compute four important quantities: the instantaneous Earth-relative position of the spacecraft, $r_{ECEF}(t)$, the instantaneous Earth-relative velocity of the spacecraft, $v_{ECEF}(t)$, the inertial rotation rate of the local-level reference frame expressed in local-level coordinates, $w_{ll}(t)$, and the orthonormal matrix transformation from Earth-Centered Earth-Fixed (ECEF) coordinates to local-level coordinates, $A_{ll/ECEF}(t)$. These quantities vary with time as the spacecraft moves in its orbit. They also depend on the Kepler parameters of the spacecraft's orbit.

This study uses two orbital models. One is a Keplerian model that includes the secular perturbations due to the Earth's J_2 oblateness effect. These perturbations affect the relationship between the semi-major axis and the mean motion, and they cause precession of the line of nodes and of the perigee. This model's mathematical form is presented in the appendix of Ref. 18. The second model is a simple circular model that neglects all oblateness effects. It is used for analysis and design calculations that must execute repeatedly and, therefore, rapidly.

Nonlinear Attitude Dynamics Model
This study uses a nonlinear rigid-body attitude dynamics model in many of its simulations. This model includes effects that are not included in a simpler design model, effects such as the drag torque and the J_2 terms in the gravity gradient torque.

The nonlinear attitude model includes kinematic and dynamic equations of motion:

$$\dot{q} = \frac{1}{2}\begin{bmatrix} 0 & w_{sc/ll3} & -w_{sc/ll2} & w_{sc/ll1} \\ -w_{sc/ll3} & 0 & w_{sc/ll1} & w_{sc/ll2} \\ w_{sc/ll2} & -w_{sc/ll1} & 0 & w_{sc/ll3} \\ -w_{sc/ll1} & -w_{sc/ll2} & -w_{sc/ll3} & 0 \end{bmatrix} q \quad (2a)$$

$$I\,\dot{\boldsymbol{w}} + \boldsymbol{w}\times I\boldsymbol{w} = m\times b + n_{gg} + n_d \qquad (2b)$$

where eq. (2a) is the quaternion kinematic equation and eq. (2b) is Euler's equation of motion for a rigid body. In this model $\boldsymbol{w} = [w_1; w_2; w_3]$ is the rotation rate of the spacecraft-fixed reference frame with respect to inertial coordinates. It is expressed in the spacecraft reference frame. The vector $[w_{sc/ll1}; w_{sc/ll2}; w_{sc/ll3}] = \{\boldsymbol{w} - A_{sc/ll}(q)\boldsymbol{w}_{ll}(t)\}$ is the rotation rate of the spacecraft-fixed reference frame with respect to the local-level reference frame, expressed in spacecraft-fixed coordinates. The 3×3 I matrix is the mass moment of inertia matrix of the spacecraft. The quantity n_{gg} is the gravity gradient torque, and n_d is the net remaining disturbance torque.

The magnetic field in spacecraft coordinates, b, is computed using the spacecraft position, the spacecraft attitude, and a spherical harmonic model of the Earth's magnetic field [17]:

$$b = A_{sc/ll}(q)\, A_{ll/ECEF}(t)\, b_{ECEF}[r_{ECEF}(t),t] \qquad (3)$$

where b_{ECEF} is the Earth's field in ECEF coordinates. It is a function of spacecraft position and of time.

The gravity gradient model computes n_{gg} as a function of the spacecraft's position, attitude, and inertia matrix: $n_{gg} = n_{gg}[r_{ECEF}(t), A_{sc/ll}(q)A_{ll/ECEF}(t), I]$. This model includes the J_2 gravity gradient terms, which is why it depends on r_{ECEF}.

The disturbance model includes the aerodynamic drag torque and the effects of residual spacecraft magnetic dipole moment:

$$n_d = r_{ac}\times f_{drag} + m_{resid}\times b \qquad (4)$$

In this equation r_{ac} is the position vector of the aerodynamic center measured with respect to the center of mass, f_{drag} is the drag force, and m_{resid} is the residual magnetic dipole moment of the spacecraft. These vectors are expressed in spacecraft coordinates. The drag is

$$f_{drag} = A_{sc/ll}(q)\bullet A_{ll/ECEF}(t)\bullet$$
$$\{-0.5\,r[r_{ECEF}(t)]\,\|v_{ECEF}(t)\|\,v_{ECEF}(t)\,S\,C_D\} \qquad (5)$$

where $r[r_{ECEF}(t)]$ gives the air density as a function of altitude from the 1976 U.S. Standard Atmosphere [19], S is the spacecraft's aerodynamic reference area, and C_D is its drag coefficient. Other disturbances, such as solar radiation pressure and outgassing, have not been modeled because the two torques in eq. (4) are often the dominant attitude disturbances in low Earth orbit.

The general Kepler orbital model has been used with this nonlinear attitude dynamics model. Because it includes eccentricity and secular J_2 effects, this model is more representative of an actual orbit. This increased fidelity is consistent with the nonlinear attitude model's purpose, which is to provide a realistic evaluation of a controller design's closed-loop performance.

Linearized Attitude Dynamics Model

The high-fidelity nonlinear model in eqs. (2a) and (2b) is too complicated for use in control design or in closed-loop stability analysis. Fortunately, a simpler linearized model can accurately approximate the system over a wide range of conditions. The linearized model assumes a circular orbit, and linearization is performed about the equilibrium nadir-pointing attitude. The linearized model is:

$$
\begin{bmatrix} \dot{f} \\ \dot{q} \\ \dot{y} \\ \dot{w}_{sc/ll1} \\ \dot{w}_{sc/ll2} \\ \dot{w}_{sc/ll3} \end{bmatrix}
=
\begin{bmatrix}
0 & 0 & 0 & 1 & 0 & 0 \\
0 & 0 & 0 & 0 & 1 & 0 \\
0 & 0 & 0 & 0 & 0 & 1 \\
-4w_o^2 s_1 & 0 & 0 & 0 & 0 & w_o(1-s_1) \\
0 & 3w_o^2 s_2 & 0 & 0 & 0 & 0 \\
0 & 0 & w_o^2 s_3 & -w_o(1+s_3) & 0 & 0
\end{bmatrix}
\begin{bmatrix} f \\ q \\ y \\ w_{sc/ll1} \\ w_{sc/ll2} \\ w_{sc/ll3} \end{bmatrix}
$$

$$
+
\begin{bmatrix}
0 & 0 & 0 \\
0 & 0 & 0 \\
0 & 0 & 0 \\
0 & b_3(t)/I_{11} & -b_2(t)/I_{11} \\
-b_3(t)/I_{22} & 0 & b_1(t)/I_{22} \\
b_2(t)/I_{33} & -b_1(t)/I_{33} & 0
\end{bmatrix}
\begin{bmatrix} m_1 \\ m_2 \\ m_3 \end{bmatrix}
+
\begin{bmatrix}
0 & 0 & 0 \\
0 & 0 & 0 \\
0 & 0 & 0 \\
1/I_{11} & 0 & 0 \\
0 & 1/I_{22} & 0 \\
0 & 0 & 1/I_{33}
\end{bmatrix}
n_d \qquad (6)
$$

In these equations f, q, and y are the roll, pitch, and yaw angles, respectively, and w_o is the orbital rate. I_{ii} is the moment of inertia of the spacecraft about its *ith* principal axis, and $s_i = (I_{jj} - I_{kk})/I_{ii}$ for the (i,j,k) index sets $(1,2,3)$, $(2,3,1)$ and $(3,1,2)$. $b_i(t)$ is the *ith* component of the Earth's magnetic field vector in local-level coordinates, and m_i is the *ith* component of the spacecraft torquers' induced magnetic dipole moment in spacecraft coordinates. To first order in the roll, pitch, and yaw angles, the attitude quaternion is q $\cong [0.5f; 0.5q; 0.5y; 1]$.

The model in eq. (6) includes gravity-gradient effects, gyroscopic effects, magnetic control torques, and disturbance torques, just as in the nonlinear model in eqs. (2a) and (2b). Besides linearization, the only other simplification in eq. (6) is that the J_2 gravity gradient effects have been neglected.

This model assumes that the nominal nadir-pointing spacecraft axes are principal axes. This assumption can be relaxed. In that case the disturbance torque, n_d, will include some constant gravity gradient effects, and the matrices in eq. (6) will change to include the effects of cross products of inertia.

This model is in the general time-varying linear system form:

$$\dot{x} = A x + B(t) u + B_w w \qquad (7)$$

where $x = [f; q; y; w_{sc/ll1}; w_{sc/ll2}; w_{sc/ll3}]$ is the state vector, $u = m$ is the control vector, and $w = n_d$ is the disturbance vector. The matrices A, $B(t)$, and B_w are effectively defined by eq. (6). Note that only the control effectiveness matrix, $B(t)$, is time varying. Its time variations come from the time variations of the magnetic field components, $b_i(t)$ for $i = 1$, 2, and 3.

The time variations of this system can be approximated as being periodic: $b(t) = b(t+T)$ where $T = 2p/w_o$ is the orbital period. True periodicity would hold if the Earth did not rotate and if the orbit did not precess. Earth rotation and orbit precession cause small deviations from this assumption because of asymmetries in the Earth's magnetic field. The principal asymmetry is the cant of the main dipole slightly away from the Earth's rotation axis.

A dipole approximation of the Earth's magnetic field, when coupled with the assumptions of no Earth rotation and no orbit precession, yields the following periodic model for the magnetic field vector as expressed in local-level coordinates:

$$\begin{bmatrix} b_1(t) \\ b_2(t) \\ b_3(t) \end{bmatrix} = \frac{m_f}{a^3} \begin{bmatrix} cos\,w_0 t\,sin\,i_m \\ -cos\,i_m \\ 2\,sin\,w_0 t\,sin\,i_m \end{bmatrix} \qquad (8)$$

where i_m is the inclination of the spacecraft's orbit with respect to the magnetic equator and a is the orbit's semi-major axis. Time is measured from $t = 0$ at the ascending-node crossing of the magnetic equator. The field's dipole strength is $m = 7.9 \times 10^{15}$ Wb-m.

III. Periodic Linear Quadratic Regulator Design in the Low-Bandwidth Asymptotic Limit

Rationale

Suppose one is given the periodic LQR problem:

find: $\quad u(t)$ for $0 \le t \le T \qquad (9a)$

to minimize: $\quad J = \frac{1}{2} \int_0^T \left\{ x^T(t) Q\, x(t) + u^T(t) R u(t) \right\} dt$

$$+ \frac{1}{2} x^T(T) P_T\, x(T) \qquad (9b)$$

subject to: $\quad \dot{x} = A x + B(t) u \qquad (9c)$

$\qquad\qquad\quad x(0)$ given $\qquad (9d)$

where Q and R are constant weighting matrices, P_T is the terminal state weighting matrix, and $B(t)$ is assumed to be exactly periodic, i.e., $B(t) = B(t+T)$. It is well known that the solution to this problem can be expressed in the form of a feedback control law: $u(t) = -R^{-1}B^T(t)P(t)x(t)$ where $P(t)$ is the solution of a time-varying matrix Riccati equation. Furthermore, for an appropriately chosen P_T, the resulting $P(t)$ is periodic with period T. This is equivalent to the infinite horizon solution and leads to a periodic gain, $K(t) = K(t+T) = R^{-1}B^T(t)P(t)$.

A control law of this form is very useful in the context of magnetic-torquer-based attitude control. Instead of computing a periodic gain matrix time history, $K(t)$, it is better to express the gain as $R^{-1}B^T(t)P(t)$. In this case, one can take advantage of the fact that the $B(t)$ matrix of eq. (6) can be computed from magnetometer measurements of $b(t)$ and knowledge of the spacecraft inertia matrix. This allows the computed gain to compensate for uncertainty in the Earth's magnetic field.

The control law $u(t) = -R^{-1}B^T(t)P(t)x(t)$ would be even more attractive for use in a real system if $P(t)$ were a constant matrix, i.e., if $P(t) = P_{ss}$. A constant P_{ss} would be much easier to store than a whole matrix time history. Furthermore, a constant P_{ss} would not need to have its time variations synchronized with the actual time variations in $B(t)$. As already noted, the true $B(t)$ is not exactly periodic. Therefore, synchronization of a periodic $P(t)$ with the quasi-periodic $B(t)$ could be difficult. The same would go for a controller that lumped R^{-1}, $B^T(t)$, and $P(t)$ together into the periodically time-varying gain $K(t)$.

In summary, this paper envisions a control law of the form $u(t) = -R^{-1}B^T(t)P_{ss}x(t)$. The only time-varying component of its gain is the matrix $B(t)$. $B(t)$ is constructed from magnetometer measurements according to its formula in eq. (6). The matrix P_{ss} is

4

(approximately) the solution to a periodically time-varying matrix Riccati equation, but it happens to be constant. The next sub-section will demonstrate conditions under which such a P_{ss} exists.

This control law is somewhat similar to that of Ref. 7. If R is a scaled identity matrix, then multiplication by $R^{-1}B^T(t)$ projects the control input perpendicular to the local magnetic field. This projection is accomplished by forming a cross product with the field vector, as in Ref. 7.

Asymptotic Analysis of a Low-Bandwidth Solution to a Periodic Matrix Riccati Equation

The $P(t)$ matrix is the solution of the following time-varying matrix Riccati equation:

$$\dot{P}(t) = -P(t)A - A^T P(t) - Q + P(t)B(t)R^{-1}B^T(t)P(t) \tag{10}$$

For an infinite-horizon problem, the steady-state solution can be found by imposing the following periodic boundary condition: $P(0) = P(T)$.

Theorem. If the following conditions are met:

a) $R = R_0/e^2$ where R_0 is positive definite.

b) $[A, \tilde{B}_0]$ is stabilizable where

$$\tilde{B}_0 \tilde{B}_0^T = \frac{1}{T}\int_0^T B(t)R_0^{-1}B^T(t)dt \text{ by definition.}$$

c) $[A, C]$ is observable, where $C^TC = Q$ by definition.

d) A has no eigenvalues in the right-half plane.

e) Every eigenvalue of A is unique; i.e., there are no repeated eigenvalues.

then $P(t) \to P_{ss}$, a constant matrix, in the limit as the control weighting goes to infinity, i.e., as $e \to 0$. Note that condition (e) allows A to have complex conjugate pairs of eigenvalues.

Proof. The proof uses a combined Fourier and asymptotic series representation of $P(t)$. Start by expressing $P(t)$ and $B(t)R_0^{-1}B^T(t)$ as Fourier series:

$$P(t) = P_0 + \sum_{k=1}^{\infty}\left\{P_{ck}\cos\left(\frac{2pkt}{T}\right) + P_{sk}\sin\left(\frac{2pkt}{T}\right)\right\} \tag{11a}$$

$$B(t)R_0^{-1}B^T(t) = \tilde{B}_0\tilde{B}_0^T +$$
$$\sum_{k=1}^{\infty}\left\{BRB_{ck}\cos\left(\frac{2pkt}{T}\right) + BRB_{sk}\sin\left(\frac{2pkt}{T}\right)\right\} \tag{11b}$$

This is possible because these two matrix time histories are periodic. The matrices P_0, P_{ck}, P_{sk}, BRB_{ck}, and BRB_{sk} are constant Fourier coefficients.

Next, express the Fourier coefficients of $P(t)$ as asymptotic series in the small quantity e:

$$P_0 = e^{-1}P_{0(-1)} + P_{0(0)} + e P_{0(1)} + e^2 P_{0(2)} + \dots \tag{12a}$$

$$P_{ck} = P_{ck(0)} + e P_{ck(1)} + e^2 P_{ck(2)} + \dots$$
$$\text{for k = 1, 2, 3, …} \tag{12b}$$

$$P_{sk} = P_{sk(0)} + e P_{sk(1)} + e^2 P_{sk(2)} + \dots$$
$$\text{for k = 1, 2, 3, …} \tag{12c}$$

Next, perform an asymptotic decomposition of eq. (10) followed by a Fourier decomposition. Substitute eqs. (12a)-(12c) into eqs. (11a) and (11b) and substitute the results into eq. (10). Asymptotic analysis dictates that the sum of the coefficients of e^j on the right-hand side of the equation must equal the sum of the coefficients of e^j on the left-hand side of the equation for all $j = -1, 0, 1, 2, \dots$ Fourier analysis dictates that, in each of the resulting e^j equations, the sum of the coefficients of $\cos(2pkt/T)$ on the right-hand side of the equation must be equal to the sum of the coefficients of $\cos(2pkt/T)$ on the left-hand side. The same goes for the constant terms and for the sums of the coefficients of $\sin(2pkt/T)$.

If one recognizes that $R^{-1} = e^2 R_0^{-1}$, then this matching of powers of e and of cosine, sine, and constant terms yields the following relationships:

e^{-1} eq., constant terms:
$$0 = -P_{0(-1)}A - A^T P_{0(-1)} \tag{13a}$$

e^0 eq., constant terms:
$$0 = -P_{0(0)}A - A^T P_{0(0)} - Q + P_{0(-1)}\tilde{B}_0\tilde{B}_0^T P_{0(-1)} \tag{13b}$$

e^0 eq., $\cos(2pkt/T)$ terms:
$$\frac{2pk}{T}P_{sk(0)} = -P_{ck(0)}A - A^T P_{ck(0)} + P_{0(-1)}BRB_{ck}P_{0(-1)} \tag{13c}$$

e^0 eq., $\sin(2pkt/T)$ terms:
$$-\frac{2pk}{T}P_{ck(0)} = -P_{sk(0)}A - A^T P_{sk(0)} + P_{0(-1)}BRB_{sk}P_{0(-1)} \tag{13d}$$

The remainder of this proof will show that, if $P_{ss} = e^{-1}P_{0(-1)} + P_{0(0)}$, then $\|P(t)x - P_{ss}x\|$ is on the order of $e\|P(t)x\|$. This is a good working definition of equivalence between $P(t)$ and P_{ss} as $e \to 0$ because it implies that u from the approximate control law, $u = -R^{-1}B^T(t)P_{ss} x$, will approach the exact LQR feedback control, $u = -R^{-1}B^T(t)P(t) x$, as $e \to 0$.

Assume, without loss of generality, that A has been diagonalized and that the first p diagonal elements are the neutrally stable eigenvalues of A: $A = \text{diag}(l_1, l_2, l_3, \dots, l_n)$, where $\text{real}(l_i) = 0$ for $i = 1, \dots, p$ and $\text{real}(l_i) < 0$ for $i = (p+1), \dots, n$. Diagonalization of A is possible because of the assumption (e) of the theorem.

Making use of the diagonal form of A, eq. (13a) becomes

$$0 = \begin{bmatrix} \{P_{0(-1)}\}_{11}(\bar{l}_1 + l_1) & \cdots & \{P_{0(-1)}\}_{1n}(\bar{l}_1 + l_n) \\ \vdots & \ddots & \vdots \\ \{\bar{P}_{0(-1)}\}_{1n}(\bar{l}_n + l_1) & \cdots & \{P_{0(-1)}\}_{nn}(\bar{l}_n + l_n) \end{bmatrix} \tag{14}$$

where $\{P_{0(-1)}\}_{ij}$ is the i-j element of $P_{0(-1)}$ and the bar overstrike denotes complex conjugation. Note that the matrix transpose operation includes complex conjugation.

Equation (14) implies that the only non-zero elements of $P_{0(-1)}$ are $\{P_{0(-1)}\}_{ii}$ for $i = 1, \ldots, p$. This is true because $(\bar{I}_i + I_j)$ is nonzero except when $i = j \leq p$. The nonzero elements are the diagonal elements that are associated with the neutrally stable eigenvalues of A.

The nonzero $\{P_{0(-1)}\}_{ii}$ values can be deduced from eq. (13b):

$$\{P_{0(-1)}\}_{ii} = \sqrt{\frac{Q_{ii}}{\{\tilde{B}_0\tilde{B}_0^T\}_{ii}}} \qquad \text{for } i = 1, \ldots, p \qquad (15)$$

where $\{\tilde{B}_0\tilde{B}_0^T\}_{ii}$ is the ith diagonal element of the matrix $\tilde{B}_0\tilde{B}_0^T$. Equation (15) holds because $\{P_{0(0)}A + A^TP_{0(0)}\}_{ii} = 0$ for $i = 1, \ldots, p$, as in eq. (14). Assumption (b) of the theorem guarantees that these $\{\tilde{B}_0\tilde{B}_0^T\}_{ii}$ values are positive, and assumption (c) ensures that Q_{ii} is positive. Therefore, all of these $\{P_{0(-1)}\}_{ii}$ values are guaranteed to be positive real numbers.

Equation (13b) can also be used to compute all of the elements of $P_{0(0)}$ except for its first p diagonal elements. This fact is implied by reasoning which is similar to the reasoning that has been applied to eq. (14). The fact that $\{P_{0(-1)}\}_{ij} = 0$ if either i or j is greater than p, when coupled with assumption (c) of the theorem, implies that the lower-right $(n-p)\times(n-p)$ block of $P_{0(0)}$ is positive definite. This is the block of $P_{0(0)}$ that is associated with the stable subspace of A. It is positive definite because it is the solution of a Lyapunov equation for a stable (sub-) system.

Equations (13c) and (13d) can be used to show that $\{P_{ck(0)}\}_{ij} = 0$ and $\{P_{sk(0)}\}_{ij} = 0$ if either i or j is greater than p. Because $\{P_{0(-1)}\}_{ij} = 0$ in this case, eqs. (13c) and (13d) can be written in scalar component form as follows:

$$\frac{2pk}{T}\{P_{sk(0)}\}_{ij} = -\{P_{ck(0)}\}_{ij}(\bar{I}_i + I_j)$$

$$\text{for all } i \text{ and } j \text{ such that } i > p \text{ or } j > p \quad (16a)$$

$$-\frac{2pk}{T}\{P_{ck(0)}\}_{ij} = -\{P_{sk(0)}\}_{ij}(\bar{I}_i + I_j)$$

$$\text{for all } i \text{ and } j \text{ such that } i > p \text{ or } j > p \quad (16b)$$

This pair of homogeneous linear algebraic equations has the unique solution $\{P_{ck(0)}\}_{ij} = 0$ and $\{P_{sk(0)}\}_{ij} = 0$ if and only if

$$\begin{vmatrix} \frac{2pk}{T} & (\bar{I}_i + I_j) \\ (\bar{I}_i + I_j) & -\frac{2pk}{T} \end{vmatrix} \neq 0 \qquad (17)$$

It is straightforward to show that this determinant is nonzero if $\text{real}(I_i + I_j) < 0$, which is implied by assumption (d) of the theorem coupled with the condition that $\max(i,j) > p$.

It is now possible to conclude the proof of the theorem. Suppose that $P_{AA(-1)}$ is the $p \times p$ upper left-hand block of $P_{0(-1)}$. Similarly, suppose that $P_{AA(0)}$ is the $p \times p$ upper left-hand block of $P_{0(0)}$, that $P_{AB(0)}$ is the $p \times (n-p)$ upper right-hand block of $P_{0(0)}$, and that $P_{BB(0)}$ is the $(n-p) \times (n-p)$ lower right-hand block of $P_{0(0)}$. Then the forgoing analysis has demonstrated that

$$P(t) = \begin{bmatrix} \frac{1}{e}P_{AA(-1)} + P_{AA(0)} + \mathsf{O}(1) & P_{AB(0)} + \mathsf{O}(e) \\ P_{AB(0)}^T + \mathsf{O}(e) & P_{BB(0)} + \mathsf{O}(e) \end{bmatrix}$$

$$(18)$$

where the notation $\mathsf{O}(e^j)$ denotes an expression whose highest power of e is the jth power. Using this formula for $P(t)$ and the fact that $P_{AA(-1)}$ and $P_{BB(0)}$ are both positive definite, it is straightforward to show that $\|P(t)x - P_{ss}x\|$ is $\mathsf{O}(e\|P(t)x\|)$ for all $x \neq 0$, which is the effective definition of equivalence between $P(t)$ and P_{ss}, as previously discussed. Note that

$$P_{ss} = \begin{bmatrix} \frac{1}{e}P_{AA(-1)} + P_{AA(0)} & P_{AB(0)} \\ P_{AB(0)}^T & P_{BB(0)} \end{bmatrix} \qquad (19)$$

If x has a component in the neutrally stable subspace of A, i.e., if any of the first p elements of x are nonzero, then $\|P(t)x - P_{ss}x\|$ is $\mathsf{O}(1)$ and $\|P(t)x\|$ is $\mathsf{O}(e^{-1})$. Otherwise, $\|P(t)x - P_{ss}x\|$ is $\mathsf{O}(e)$ and $\|P(t)x\|$ is $\mathsf{O}(1)$. Taken together, these two facts imply the desired equivalence condition.

Remarks about the Theorem. It is probably possible to relax assumption (e) of the theorem. If the modified theorem is true, then its proof is more complicated, especially if some of the repeated eigenvalues of A are on the imaginary axis. In this case, the lowest power of e that appears in the asymptotic expansion of P_0 is $e^{-(2-(1/l))}$, where l is the maximum number of repetitions of an eigenvalue that is on the imaginary axis.

Computational experience with this technique demonstrates that the method works when there are repeated eigenvalues on the imaginary axis. In fact, it even seems to work if some of the eigenvalues of A are unstable, so long as they are near the imaginary axis.

The key idea of this theorem is that the closed-loop system responds relatively slowly compared to the system periodicity, T. In this case, $P(t)$ does not vary rapidly over one period. Therefore, it cannot vary much from its average value, which is P_{ss}.

A Practical Method for Computing P_{ss}. A slightly different approximation of the matrix P_{ss} can be determined by solving the following steady-state

time-invariant Riccati equation:

$$0 = -P_{ss}A - A^T P_{ss} - Q + P_{ss}\{e\tilde{B}_0\}\{e\tilde{B}_0\}^T P_{ss} \qquad (20)$$

This equation can be solved using standard software packages. Note that the control effectiveness matrix is $\{e\tilde{B}_0\}$, and the control cost weighting matrix is an identity matrix. From assumptions (a) and (b) of the theorem, it is possible to calculate $\{e\tilde{B}_0\}$ from a square root factorization of the average weighted square of $B(t)$:

$$\{e\tilde{B}_0\}\{e\tilde{B}_0\}^T = \tfrac{1}{T}\int_0^T B(t)R^{-1}B^T(t)dt \qquad (21)$$

The square root factorization of the integral can be computed using an eigenvalue decomposition. Note that the rank of $\{e\tilde{B}_0\}$ may be greater than the instantaneous rank of $B(t)$. This is true in the magnetic torque attitude control problem.

An asymptotic analysis of this P_{ss} shows that $\|\{e^{-1}P_{0(-1)} + P_{0(0)}\}x - P_{ss}x\|$ is on the order of $e\|\{e^{-1}P_{0(-1)} + P_{0(0)}\}x\|$, which means that, for small e, the new form of P_{ss} is equivalent to the form used in the proof. This analysis expands the new P_{ss} in an asymptotic series in e that is like the asymptotic expansion in eq. (12a). It then derives equations for the coefficients of this series. The first two of these equations are like eqs. (13a) and (13b). The remaining details of this analysis are straightforward, and they have been omitted for the sake of brevity.

This controller design technique is similar to the technique that is employed in Ref. 11 for its constant gain algorithm. There are two main differences. First, Ref. 11 squares the $B(t)$ control effectiveness matrix twice, once before averaging and once when it gets used in the time-invariant Riccati equation. Second, Ref. 11 makes no attempt to relate the solution of its time-invariant LQR problem to the asymptotic low-bandwidth solution of a periodically time-varying problem. This relationship can be an important aid to the development of a method for dealing with actuator saturation.

After-the-Fact Floquet Analysis. It is a good idea to check the stability of the resulting closed-loop system. The theorem only says things about the limiting small e behavior of the system. It says nothing about what constitutes "small." It may be possible to use a rather "large" e and achieve good performance. If it remains stable, then the system response is likely to be faster for a larger value of e because this involves less control weighting.

The best way to design this type of control law is to pick the LQR weighting matrices Q and R, compute P_{ss}, evaluate the closed-loop stability, and tune R

accordingly. If the system is unstable, then R must be increased. The closed-loop system model is: $\dot{x} = \{A - B(t)R^{-1}B^T(t)P_{ss}\}x$. This is a periodic model, and its stability can be evaluated via Floquet analysis [20]. Floquet stability analysis computes a state transition matrix for one period of the system and verifies that all of its eigenvalues have complex magnitude less than unity. One can use Floquet analysis to tune Q and R. One might optimize the speed of response by minimizing the maximum magnitude of the eigenvalues of the closed-loop state transition matrix.

System Robustness

Such systems can be expected to have a degree of robustness with respect to system modeling errors. This is true because the controllers are approximately full-state feedback linear quadratic regulators. Time-invariant full-state feedback LQRs are known to possess certain robustness properties [21]. This robustness should carry over into the low-bandwidth time-varying case because it is similar to a time-invariant system. In the case of the magnetic-torquer-based attitude controller, there is even more reason to expect robustness. In that case, the $B^T(t)$ matrix that is used in the control law is derived from magnetometer data; therefore, it contains very little modeling error.

Design for Control Saturation

Control saturation occurs when any component of the computed u vector exceeds the maximum that is permitted by the actuators, i.e., $|(u)_i| > (u_{max})_i$ for some i. Any practical controller must be designed to behave stably if this occurs. It is not always obvious how best to deal with this situation, especially if the feedback controller includes integrators.

Reference 22 presents a method for dealing with control saturation in the context of time-invariant LQR controllers. Its approach exploits the fact that an LQR-based controller has infinite gain margin. That is, if the control law $u = -Kx$ stabilizes the system and if K has been computed by solving an LQR problem, then the control law $u = -aKx$ will also stabilize the system for any positive scalar a in the range $0.5 < a < \yen$. For all $a > 1$ the modified controller is the solution to a modified LQR problem.

Reference 22 designs an initial LQR that has a very low bandwidth. If the system has no open-loop eigenvalues in the right-half plane, then K can be made arbitrarily small by this method, and the nominal LQR control law can be made to function stably in an arbitrarily large region of state space without violating any of the limits $|(u)_i| \leq (u_{max})_i$. Unfortunately, the resulting controller will have poor performance close to the origin of the state space because u will be very small in this region.

7

The technique goes on to use the infinite gain margin of the LQR in order to recover good performance near the equilibrium. It does this by scaling the control law by a factor $a \geq 1$. It first tries a nominal value of a that is much larger than 1, call this a_0. If this produces a control input that does not violate any of the bounds $|(u)_i| \leq (u_{max})_i$, then a_0 is used. Otherwise, it scales a down from a_0 until all of the feedback control inputs respect all of the saturation bounds.

This same technique can be used for the problem at hand. A time-varying LQR of the form $u = -K(t)x$ has the same gain margin as a time-invariant LQR. For any $a > 1$, a modified time-varying control law of the form $u = -aK(t)x$ will be the solution to a modified time-varying LQR problem and will stabilize the system. In order to design its control saturation logic, the asymptotic periodic LQR starts by using a very large R matrix in its design. This yields a P_{ss} matrix and a control law $u = -R^{-1}B^T(t)P_{ss}x$ that satisfies the no-control-saturation criterion in a very large region of state space. In order to speed the system response near the state space origin, the control law scales up the gain according to the following rules:

$$u_{nom} = -a_0 R^{-1}B^T(t)P_{ss}x \tag{22a}$$

$$b = \max_i \frac{|(u_{nom})_i|}{(u_{max})_i} \tag{22b}$$

$$u = \begin{cases} u_{nom} & \text{if } b \leq 1 \\ \frac{1}{b}u_{nom} & \text{if } 1 < b \end{cases} \tag{22c}$$

where $a_0 > 1$ is the scaling factor that increases the response speed near the equilibrium, and b is an inverse scaling factor that kicks in if saturation occurs. Using Lyapunov techniques like those of Ref. 22, the "sped-up" system with its saturation logic can be shown to be stable for the same large region of state space that is guaranteed to be stable if the slow controller is used.

IV. Application to the Magnetic Torquer Attitude Control Problem

The asymptotic periodic LQR technique has been applied to the magnetic-torquer-based attitude control design problem. This section describes how it has been applied, and it presents analysis and simulation results for two different spacecraft configurations.

Incorporation of Integrators in the Design

Integrators are often used in feedback control systems. They can eliminate the steady-state effects of constant disturbances. For the magnetic attitude control problem, the use of integrators is challenging because of the system's time-variations and especially because of the under-actuation issue: One cannot totally counteract the effects of a constant 3-axis disturbance torque because the magnetic toque is constrained to be perpendicular to the Earth's field. Nevertheless, integrators are useful because they enable the controller to counteract the average effects of any 3-axis disturbance torque. This feature eliminates pointing biases from the system.

Integrators can be added to the controller via state augmentation. Suppose that $x_{aug} = [z; x]$, where x is the 6×1 state vector associated with the linear model in eqs. (6) and (7) and z is a 3×1 vector of integrals of the attitude errors: $z_i(t) = \int^t x_i(t)dt$ for $i = 1, 2, 3$. Then the augmented state space model takes the form:

$$\dot{x}_{aug} = \begin{bmatrix} 0 & [I_{3\times 3},0] \\ 0 & A \end{bmatrix} x_{aug} + \begin{bmatrix} 0 \\ B(t) \end{bmatrix} u + \begin{bmatrix} 0 \\ B_w \end{bmatrix} w \tag{23}$$

where the matrices A, $B(t)$, and B_w are the same as in eqs. (6) and (7). This system is a periodic time-varying linear system of the same form as in eq. (9c). Although assumption (e) of the theorem is violated by the repeated eigenvalues at the origin, computational experience has shown that this system admits the design of asymptotic low-bandwidth periodic LQR controllers.

Nominal Controller Designs for two Different Spacecraft Configurations

Configuration A. The first spacecraft for which a controller has been designed has 3-axis gravity gradient stability. It's inertia matrix is $I = \text{diag}(8.7, 10, 6.5)$ kg-m^2. It is a box of dimension 0.7 m along the roll axis, 0.6 m along the pitch axis, and 0.9 m along the yaw axis. Its orbit is circular with an altitude of 600 km and an inclination of 90 deg.

An asymptotic periodic controller has been designed for this spacecraft. It uses the design that accounts for control saturation. Its slow LQR controller, the one that gets used when far from the equilibrium, has been designed using the following cost weighting matrices:

$$Q = \text{diag}(1.5\times 10^{-8}, 1.5\times 10^{-7}, 1.5\times 10^{-8}, 0.1, 1.0, 0.1, 0.1, 1.0, 0.1) \tag{24a}$$

$$R = \text{diag}(6.2\times 10^7, 6.2\times 10^7, 6.2\times 10^7) \tag{24b}$$

The units of Q are: $1/(\text{rad-sec})^2$ for the first 3 diagonal elements, $1/\text{rad}^2$ for the middle 3 diagonal elements, and $(\text{sec/rad})^2$ for the last 3 diagonal elements. The units of R are all $1/(\text{amp-m}^2)^2$. During unsaturated operation, when operating near the nadir-pointing equilibrium, fast controller response is achieved by scaling up the slow-controller's gain by the factor $a_0 = 2,500$.

The fast response of this periodic system is good. Its one-orbit state transition matrix has a maximum eigenvalue magnitude of 0.57. This translates into a settling time constant of 1.8 orbits, which means that all transients will settle to less than 2% of their initial values in about 7 orbits if control saturation does not occur. The motion associated with this slowest transient response is primarily coupled roll and yaw. This design has been optimized in the sense that a_0, the scalar gain, has been chosen so as to minimize the upper bound on the absolute values of the eigenvalues of the closed-loop system's one-orbit state transition matrix.

The eigenvalues of the actual system state transition matrix are relatively near to those of the state transition matrix for the averaged time-invariant closed loop system whose LQR solution was used to determine P_{ss}. Recall that this time-invariant system is the one whose Riccati equation appears as eq. (20). This nearness of eigenvalues demonstrates that the time-invariant averaged model is a reasonably good approximation of the time-varying system when the closed-loop time constants are on the order of one or two orbits.

Configuration B. The spacecraft for this second case has roll and pitch gravity gradient stability, but its yaw motion is neutrally stable. It's inertia matrix is $I = \mathrm{diag}(250, 250, 10)$ kg-m^2, and its rectangular form has roll, pitch, and yaw dimensions of 0.5 m, 0.5 m, and 3.4 m, respectively. It is in a circular orbit with an inclination of 57 deg and an altitude of 657 km. It is like the spacecraft that was considered in Ref. 7. The weights that have been used to design its slow LQR controller are

$$Q = \mathrm{diag}(1.5\times10^{-8}, \ 1.5\times10^{-8}, \ 1.5\times10^{-8}, \ 0.01, \ 0.01, \ 0.01, \ 1.0, 1.0, 1.0) \quad (25a)$$

$$R = \mathrm{diag}(4.9\times10^4, 4.9\times10^4, 4.9\times10^4) \quad (25b)$$

where the units in eqs. (25a) and (25b) are the same as in eqs. (24a) and (24b). The scale-up factor that it uses to achieve fast control response near the equilibrium is $a_0 = 8{,}130$.

This system is not quite as fast as the other one. The maximum eigenvalue magnitude for its one-orbit state transition matrix is 0.76. This translates into a slowest time constant of 3.7 orbits and an upper bound on its 2% settling time of about 14 orbits. Similar to Case A, the slowest mode is primarily roll-yaw motion. In contrast to Case A, the actual periodic system's state transition matrix eigenvalues are not as similar to those of its time-invariant approximation, and the value of a_0 is not quite optimized to minimize the worst-case settling time – the optimal a_0 would be about 16,000 in this case.

Robustness with Respect to Parametric System Uncertainty

An important aspect of any controller design is its tolerance of uncertainty in the open-loop system model that has been used to design it. This is especially so in the present situation. Simplifying assumptions have been made about the magnetic field model, yet under-actuation causes the controller to rely on model predictions about the field's future pointing directions.

Stability robustness has been investigated by calculating the system state transition matrix for various cases that involve model error. The one-orbit state transition matrix is calculated for the closed-loop system model $\dot{x} = \{A_{truth} - B_{truth}(t)R^{-1}B_{mixed}(t)P_{ss}\} \ x$. The matrices A_{truth} and $B_{truth}(t)$ are defined by the true orbit, the true spacecraft inertial properties, and the true magnetic field. The $B_{mixed}(t)$ matrix time history is based on the true magnetic field and the controller design model of the spacecraft inertial properties; this is consistent with the assumption that magnetometer measurements and an inertial model will be used to construct $B_{mixed}(t)$ on orbit. The P_{ss} matrix is the result of design calculations that use the matrices A_{model} and $B_{model}(t)$, which are based solely on the design model of the orbit, the spacecraft inertial properties, and the magnetic field.

Various types of parametric uncertainty between the model and the true system have been investigated. The orbital altitude has been perturbed ± 100 km. The orbital inclination has been perturbed ± 30 deg for the Case-A system and ± 20 deg for the Case-B system – this latter system should not be expected to work for inclination perturbations that make its inclination too low because the system becomes uncontrollable in pitch at zero inclination. Perturbations in the overall inertia levels of ± 30 % have been tried. Also tested have been perturbations in the ratios of principal inertias that range up to ± 25 %. Some of the Case-B inertia ratio perturbations were large enough to destabilize the open-loop system.

This study has considered two types of discrepancy between the modeled and truth magnetic fields. One is a perturbation in its period of up to ± 7%. This is representative of one of the effects of Earth rotation. The other discrepancy is an addition of higher harmonics to the truth field model. Fourier terms out to 5 times the orbital frequency have been added. Although not taken directly from a spherical harmonic Earth magnetic field model, these terms have been sized to approximate the effects of the higher harmonics that exist in the Earth's field.

Both systems exhibit robust stability for all of the parameter sets that have been considered, 16 sets per case. In all mis-modeling situations, the fast-system closed-loop state transition matrix is stable – recall that the fast system is the one that uses a_o to speed up the response. The slow system, the effective system when large amplitude response causes extreme control saturation, is stable for most of the parameter sets that have been tried. For the Case-A system, the slow system is stable for all parameter variations. The Case-B system exhibits instability in 3 scenarios, but instability occurs only for very large state amplitudes that cause the inverse scaling factor b to be 127 or greater – review eqs. (22a)-(22c). One scenario is when the true altitude is 100 km higher than the modeled altitude, and the other two scenarios occur when the yaw inertia factor $s_{yaw} = (I_{roll}-I_{pitch})/I_{yaw}$ varies by ± 0.1 away from its modeled value of 0.

The bottom line on system robustness is that the system will remain stable for a wide range of orbital and inertial variations if the nominal closed-loop response has been designed to be relatively fast. When very large state perturbations cause extreme levels of control saturation to occur, then in some cases the resultant slow system will be somewhat less robust to parameter uncertainty. At these large state perturbations the system is likely to experience other problems as well, problems such as large modeling errors due to a breakdown of the linearization assumption that has been used to derive the control law.

Nonlinear Simulation Results

A number of nonlinear simulations have been run for designs A and B. The nonlinear simulations test four aspects of system performance: a) its response to the real magnetic field of the rotating Earth, which is not a dipole and which is not quite periodic, b) the effects of system nonlinearities, including the attitude kinematic and dynamic nonlinearities of eqs. (2a) and (2b) and the control saturation nonlinearity of eqs. (22a)-(22c), c) its ability to counteract disturbance torques such as those caused by the drag and by residual magnetic dipole moments, and d) the impact of small orbital perturbations such as eccentricity and the secular J_2 effect.

Both systems perform well in a wide range of situations. They both show good transient response that agrees with the predictions of their linear models when not in a saturated situation. Both systems are able to converge from initial attitude errors of over 50 deg (30 deg per axis). These large initial conditions test both the functioning of the control saturation logic and the efficacy of linear control of this nonlinear

system. Both controllers showed good steady-state response to disturbance torques

A simulation example of the Case-A system is presented in Figs. 1 and 2. Figure 1 presents the roll, pitch, and yaw angle time histories, and Fig. 2 presents the corresponding magnetic dipole moment feedback control input time histories. This case is one that starts with a large initial attitude error, about 30 deg per axis. These large initial conditions cause controller saturation, as evidenced on Fig. 2 – the value of $u_{max} = 0.03$ amp-m^2 in this case. Nevertheless, the system successfully converges to its equilibrium response in a little more than a day.
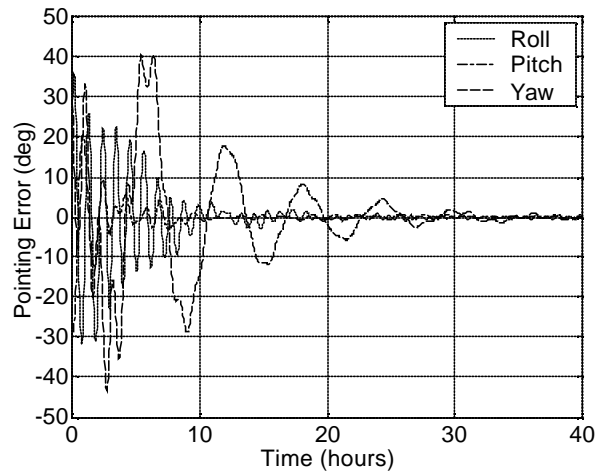

Fig. 1. System-A pointing error time histories that start with 30 deg initial errors on all 3 axes.
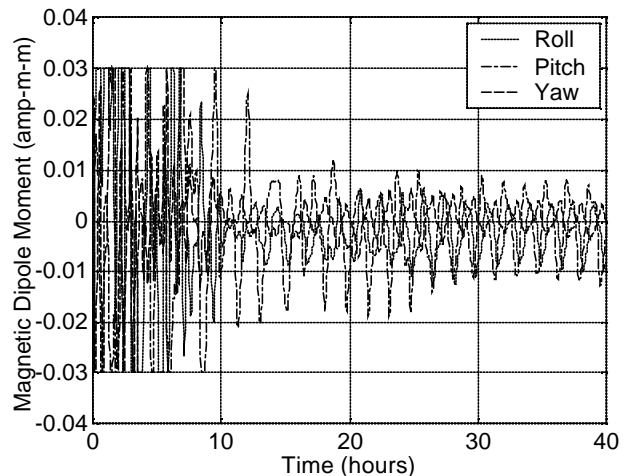

Fig. 2. Control input time histories for the system-A example that starts with 30 deg initial pointing errors on all 3 axes.

In this simulation case there are significant discrepancies between the simulation model and the

10

model that has been used to design the controller. In addition to the field model differences, there are differences in the orbit and in the spacecraft inertias. Thus, this simulation demonstrates the controller's robustness.

The residual system oscillations after 30 hours are caused by the disturbance torques. The average drag torque is 1.6×10^{-7} N-m about the pitch axis and 1.0×10^{-7} N-m about the yaw axis, which is somewhat conservative for this configuration. In addition, there are oscillatory disturbance torques from the drag (due to the orbital eccentricity of 0.002) and from a residual magnetic dipole moment. These oscillatory torques have peak-to-peak amplitudes as large as 3×10^{-7} N-m. The closed-loop steady-state response is unbiased on all 3 axes with maximum pitch and roll errors of 0.7 deg and a maximum yaw error of 1 deg. In open-loop operation, the mean drag torque alone would have produced mean roll, pitch, and yaw errors of 0 deg, 0.5 deg, and 7.8 deg, respectively. This controller greatly improves the system's yaw accuracy at the expense of slightly increased roll and pitch errors.

The response of system B to large initial errors is depicted in Fig. 3. As in Fig. 1, the initial errors are about 30 deg on all three axes. This system takes longer to settle down, but it is clearly stable. The dipole moment control input time history, not shown, displays saturated operation for the first 81 hours of this transient. The value of u_{max} is 0.1 amp-m^2 in this case. As in Fig. 2, the saturated response is oscillatory, like bang-bang control. It is remarkable that the controller converges at all in this case. Recall that the yaw mode for this design is neutrally stable. When combined with the integral action in the controller, the entire yaw subsystem is a series of 3 integrators. Such systems are very hard to stabilize when there is control saturation, even in the time-invariant case. What is more, the yaw mode's 3 repeated roots at the origin violate assumption (e) of the theorem. The ability to converge for this situation demonstrates that the proposed method is a powerful tool for attitude controller design.

System B's steady-state response to disturbances is shown in Fig. 4. This example has mean drag torques of 7.3×10^{-7} N-m about the pitch axis and 2.6×10^{-7} N-m about the yaw axis. These torques are consistent with the size of this spacecraft and its likely aerodynamic-center-to-center-of-mass offset. The maximum steady-state roll, pitch, and yaw errors are 0.6 deg, 0.4 deg, and 0.4 deg respectively. These roll and pitch errors are significantly larger than would be caused by the drag torque in an open-loop situation, but the yaw

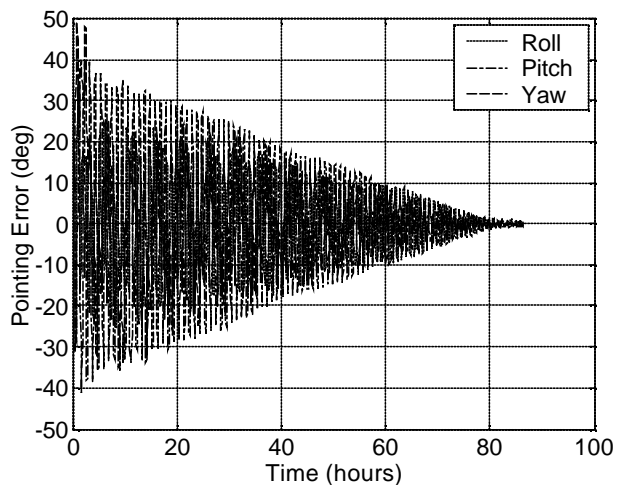error is much lower. It would be infinity in open-loop operation because the yaw mode is neutrally stable.

Fig. 3. System-B pointing error time histories that start with 30 deg initial errors on all 3 axes.
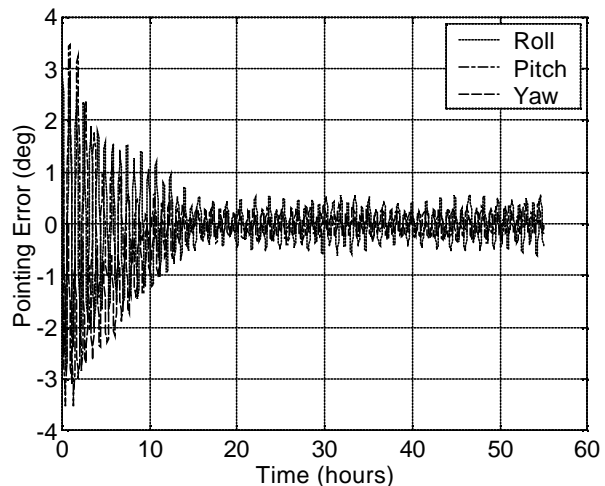

Fig. 4. Transient and steady-state pointing error time histories for system B, an example that includes an unmodeled residual magnetic dipole moment and a moderate level of drag torque based on the given spacecraft size.

Much of the oscillatory steady-state response in Fig. 4 is due to the way in which this quasi 3-axis system deals with a true 3-axis disturbance. In the process of nulling out the average effects of the constant drag torque, the controller induces oscillations. A good controller design will induce relatively small "side-effect" oscillations while it counteracts a given constant disturbance torque, but there will always be some minimum level of oscillation.

An unmodeled residual magnetic dipole moment also contributes to the steady-state attitude oscillations shown in Fig. 4. The residual dipole moment for this example has a norm of 0.016 amp-m^2, which equals 1/6 of u_{max}, and it gives rise to oscillatory disturbance torques as large as 1×10^{-6} N-m peak-to-peak. The controller is not so good at dealing with this type of oscillatory disturbance.

In principle, a magnetic-torque-based controller should be able to completely counteract this disturbance. It would need to use some sort of estimator of the residual dipole moment in order to better null out this disturbance effect. Such an addition to the controller logic might be very important because residual dipole moments can be much larger than the levels used in this study.

V. Conclusions

This paper has shown how to design a class of stabilizing attitude controllers for nadir-pointing spacecraft. These controllers use only magnetic actuation. Their control laws are designed using a new type of periodic linear quadratic regulator whose Riccati equation solution is approximated by a linear time-invariant solution for an averaged system. The resulting full-state feedback controller derives its periodicity from the time-varying control influence matrix, which can be derived from on-board magnetometer measurements. The controllers use integrators in order to counteract steady-state disturbance torques, and they employ a type of saturation logic that maintains stability by using the infinite gain margin property of linear quadratic regulators.

This technique has been applied to two example systems, both of which have only magnetic actuation and no wheels or gravity gradient booms. The controller's performance has been studied via analysis and simulation. The system has been shown to be very robust with respect to modeling errors in the magnetic field, the spacecraft inertia matrix, and the orbital properties. The system can converge from attitude errors of 30 deg per axis. It can achieve pointing accuracies on the order of 0.5 to 1.0 deg for spacecraft designs that have reasonable levels of drag torque.

This system may be an attractive alternative to a gravity gradient boom or a set of thrusters. It can provide more accuracy for less weight than can a gravity gradient system, and it does not expend fuel like a thruster system.

The techniques developed in this paper also can be applied to momentum bias systems and other similar systems. They may prove helpful in such systems by increasing the pointing accuracy or by decreasing the required wheel size for a given level of accuracy.

References

1. Psiaki, M.L., Theiler, J., Bloch, J., Ryan, S., Dill, R.W., and Warner, R.E. "ALEXIS Spacecraft Attitude Reconstruction with Thermal/Flexible Motions Due to Launch Damage", *Journal of Guidance, Control, and Dynamics*, Vol. 20, No. 5, 1997, pp. 1033-1041.

2. Fox, S.M., Pal, P.K., Psiaki, M.L., and Mook, M.E., "Magnetic Attitude Determination Subsystem Performance on the LACE Spacecraft," *Guidance and Control 1991; Proceedings of the Annual Rocky Mountain Guidance and Control Conf.*, Feb. 1991, Keystone, Colorado, pp. 553-574.

3. Iida, H. and Ninomiya, K., "A New Approach to Magnetic Angular Momentum Management for Large Scientific Satellites," *NEC Research & Development*, Vol. 37, No. 1, 1996, pp. 60-77.

4. Ferreira, L.D.D. and da Cruz, J.J., "Attitude and Spin Rate Control of a Spinning Satellite Using Geomagnetic Field," *Journal of Guidance, Control, and Dynamics*, Vol. 14, No. 1, 1991, pp. 216-218.

5. Pittelkau, M.E., "Optimal Periodic Control for Spacecraft Pointing and Attitude Determination," *Journal of Guidance, Control, and Dynamics*, Vol. 16, No. 6, 1993, pp. 1078-1084.

6. Alfriend, K.T., "Magnetic Attitude Control System for Dual-Spin Satellites," *AIAA Journal*, Vol. 13, No. 6, 1975, pp. 817-822.

7. Martel, F., Pal, P.K., and Psiaki, M.L., "Active Magnetic Control System for Gravity Gradient Stabilized Spacecraft," *Proceedings of the 2nd Annual AIAA/USU Conf. on Small Satellites*, Sept. 1988, Logan, Utah, pp. unnumbered.

8. Musser, K.L. and Ebert, W.L., "Autonomous Spacecraft Attitude Control using Magnetic Torquing Only," *Proceedings of the Flight Mechanics/Estimation Theory Symposium*, NASA Goddard Space Flight Center, Greenbelt, MD, May 1989, pp. 23-38.

9. Steyn, W.H., "Comparison of Low-Earth-Orbit Satellite Attitude Controllers Submitted to Controllability Constraints," *Journal of Guidance, Control, and Dynamics*, Vol. 17, No. 4, 1994, pp. 795-804.

10. Arduini, C. and Baiocco, P., "Active Magnetic Damping Attitude Control for Gravity Gradient

Stabilized Spacecraft," *Journal of Guidance, Control, and Dynamics*, Vol. 20, No. 1, 1997, pp. 117-122.

11. Wiśniewski, R., "Linear Time Varying Approach to Satellite Attitude Control Using Only Electromagnetic Actuation," *Proceedings of the AIAA Guidance, Navigation, and Control Conf.*, Aug. 1997, New Orleans, pp. 243-251.

12. Wang, P. and Shtessel, Y.B., "Satellite Attitude Control Using Only Magnetic Torquers," *Proceedings of the AIAA Guidance, Navigation, and Control Conf.*, Aug. 1998, Boston, pp. 1490-1498.

13. Curti, F. and Diani, F., "Study on Active Magnetic Attitude Control for Italian Spacecraft Bus MITA," Proceedings of the 14th International Conference on Space Flight Dynamics, Brazilian Space Research Center, (Iguasso Falls, Brazil, 1999). pp. unnumbered.

14. Wiśniewski, R. and Blanke, M., "Fully Magnetic Attitude Control for Spacecraft Subject to Gravity Gradient," *Automatica*, Vol. 35, No. 7, 1999, pp. 1201-1214.

15. Krishnan, H., McClamroch, N.H., and Reyhanoglu, M., "Attitude Stabilization of a Rigid Spacecraft Using Two Momentum Wheel Actuators," *Journal of Guidance, Control, and Dynamics*, Vol. 18, No. 2, 1995, pp. 256-263.

16. Morin, P. and Samson, C., "Time-Varying Exponential Stabilization of a Rigid Spacecraft with Two Control Torques," *IEEE Transactions on Automatic Control*, Vol. 42, No. 4, 1997, pp. 528-534.

17. Wertz, J.R. ed., *Spacecraft Attitude Determination and Control*, D. Reidel Pub. Co., (Boston, 1978), pp. 414, 779-786.

18. Psiaki, M.L., "Autonomous Orbit and Magnetic Field Determination Using Magnetometer and Star Sensor Data," *Journal of Guidance, Control, and Dynamics*, Vol. 18, No. 3, 1995, pp. 584-592.

19. Anon., *U.S. Standard Atmosphere, 1976*, National Oceanic and Atmospheric Administration, 1976.

20. Kailath, T., *Linear Systems*, Prentice-Hall, (Englewood Cliffs, N.J., 1980), p. 608.

21. Stengel, R.F., *Optimal Control and Estimation*, Dover, (New York, 1994), pp. 571-602.

22. Saberi, A., Lin, Z., and Teel, A.R., "Control of Linear Systems with Saturating Actuators," *IEEE Transactions on Automatic Control*, Vol. 41, No. 3, 1996, pp. 368-378.